Ultrasound in Med. & Biol. Vol. 15, No. 5, pp. 451–460, 1989
Printed in the U.S.A.

0301-5629/89 $3.00 + .00

●*Original Contribution*

HISTOPATHOLOGY OF SHOCK WAVE TREATED TUMOR CELL SUSPENSIONS AND MULTICELL TUMOR SPHEROIDS

THOMAS BRÄUNER, FRANZ BRÜMMER and DIETER F. HÜLSER
Biology Institute, Biophysics Department, University of Stuttgart, Pfaffenwaldring 57, 7000 Stuttgart 80, Federal Republic of Germany

(*Received* 20 *September* 1988; *in final form* 24 *November* 1988)

Abstract—L1210 mouse leukemia cell suspensions exposed to 500 shock waves (SW) in an experimental lithotripter (XL1, Dornier) revealed severe cellular damage. Apart from cell fragments and cellular debris, cells exhibited alterations of shape, vacuolisation of the cytoplasm, perinuclear cisternae, swelling of mitochondria or rupture of the mitochondrial fine structure, and permeabilization of the cell membrane. Treatment of multicell tumor spheroids of both HeLa and EMT6/Ro cells in suspension with 500 SW resulted either in loss of peripheral cells and serious cellular damage in the outer regions or in a fragmentation of the spheroids. Many of the geometrically intact cells exhibited the same histopathological alterations as the suspended L1210 cells. Immobilization of the spheroids in agar or gelatine, however, prevented spheroids from being agitated and accelerated during SW-exposure. After treatment with 500 SW, spheroids immobilized in gelatine were not different from control cultures, as investigated with light- and electronmicroscopy. From our results we conclude that spheroids in suspension are subject to cavitation and liquid jet formation, causing not only acceleration and shearing forces but also collisions which account for the observed cell damage.

Key Words: **Shock waves, Extracorporal shock wave lithotripsy, L1210 cells, Cell suspension, Multicell tumor spheroids, EMT6/Ro cells, HeLa cells, Immobilisation, Cavitation, Jet streams, Shearing forces, Light- and electronmicroscopical histology.**

INTRODUCTION

Extracorporal shock wave lithotripsy has become a routine clinical procedure for the non-surgical disintegration of renal and ureteral calculi. Since the first kidney stone destruction in humans by Chaussy and coworkers (1980), worldwide more than a million patients have been treated with this technology (Eisenberger 1988). The first lithotripter for routine clinical use was the model HM3 (Dornier Medizintechnik, Germering, FRG). In this instrument shock waves (SW) are generated by an underwater electrical discharge between two electrode tips located in the first focal point F_1 of a brass semi-ellipsoid. The electrical discharge gives rise to a rapidly expanding plasma which collapses, thus generating a shock wave front. Shock waves reflected from the wall of the semi-ellipsoid converge at the second focal point F_2, where a pressure peak with an amplitude of about 40 MPa (Coleman et al. 1987c) and a rise time in the nanosecond range is built up. Disintegration of the kidney stone in F_2 (Fig. 1) is thought to occur due to both pressure forces as the wave enters the stone and tensile forces as the wave is reflected at the interface between stone and tissue (Chaussy et al. 1980; Coleman et al. 1987a). Measurements with a Dornier extracorporal shock wave lithotripter, however, revealed cavitation as evidenced by liquid jet impacts on various surfaces over a volume greater than 200 cm^3 (Coleman et al. 1987b).

At the present time, it is a matter of discussion whether cavitation contributes to stone disintegration and to histopathological effects on cells. It is, however, possible that cavitation is responsible for complications (*e.g.*, subcapsular and diffuse hemorrhages) observed after both clinical shock wave application to humans (Baumgartner et al. 1987) and exposure of dogs to therapeutic shock wave doses (Delius et al. 1988).

Meanwhile, attempts have been made to utilize the observed damage to biological tissue for the suppression of tumor growth *in vitro* and *in vivo* (Russo et al. 1986). Tumor cell suspensions exposed to SW revealed severe pathological alterations including cell fragmentation, whereas treatment of the same cells grown as tumor nodules *in vivo* did not cause histo-

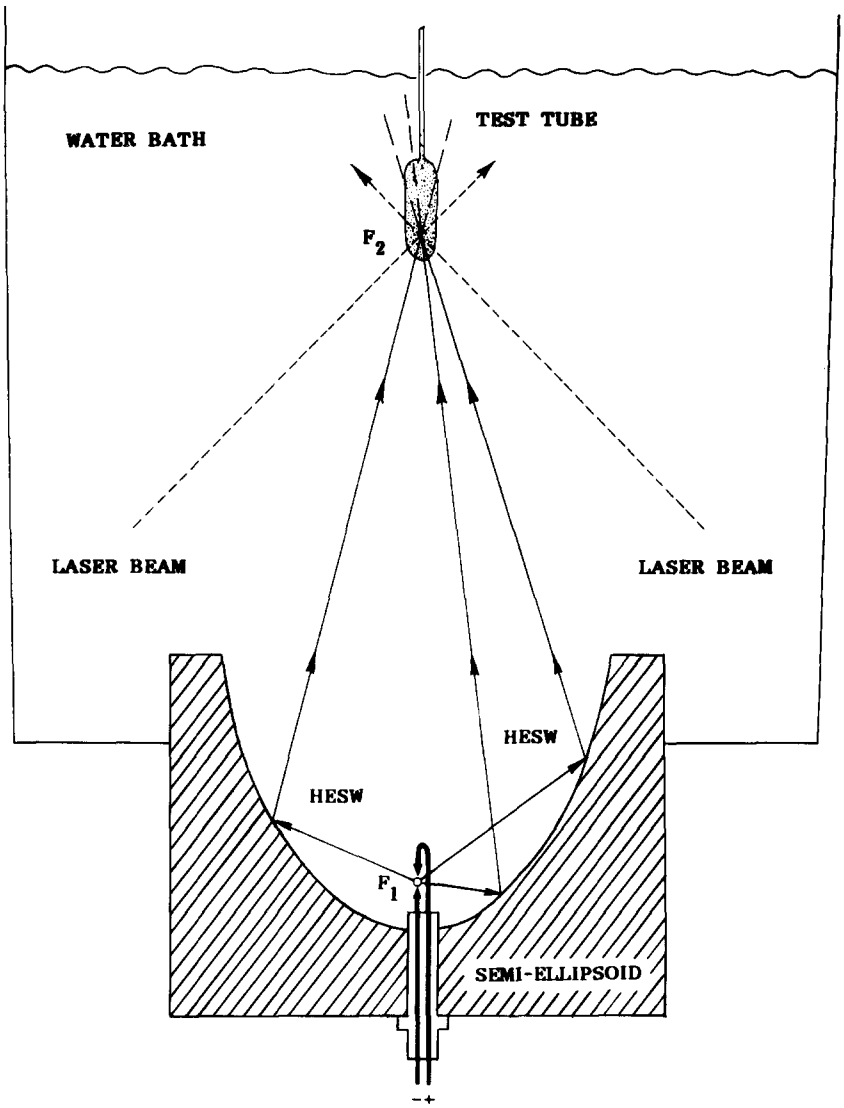

Fig. 1. Treatment of cell cultures with SW in a Dornier XL1 lithotripter. SW are generated by underwater spark discharge (18 kV, 80 nF, 1 Hz) between two electrode tips in the first focal point (F_1) of a brass semi-ellipsoid. Cell cultures are exposed to SW in polyethylene test tubes positioned in the second focal point (F_2) indicated by the cross-over of two laser beams.

pathological or ultrastructural lesions different from that observed in untreated tumors.

The aim of our study was to investigate the biological effects of SW on tumor cells under various growth and exposure conditions. Tumor cells were either treated as single cell suspensions or as multicell tumor spheroids. These multicell tumor spheroids exhibit structures analogous to those observed in the original tumor and a histological organisation similar to that of solid tumors *in vivo* (Sutherland et al. 1971). They have, therefore, been introduced as *in vitro* models of tumor microregions and of an early, avascular stage of tumor growth in various fields of experimental cancer research (reviews: Müller-Klieser 1987; Sutherland 1988).

MATERIALS AND METHODS

Cell lines

L1210 cells were derived from lymphocytic mouse leukemia cells maintained in the ascitic form in DBA/2 mice (Hutchinson et al. 1966). The epithelioid HeLa cells were established from a human cervix carcinoma (Gey et al. 1952; Scherer et al. 1953). The fibroblastioid EMT6/Ro cells were selected from a mammary tumor cell line of a Balb/c mouse (Rockwell et al. 1972).

Culture conditions

L1210 cells were cultured as single cell suspensions in tissue culture flasks (Greiner, Nürtingen, FRG). RPMI 1640 growth medium with $NaHCO_3$ (Boehringer Mannheim 209945, FRG) was supplemented with 15% fetal calf serum (Boehringer Mannheim 210471) and—prior to use—with 100 μL mercaptoethanol (0.4 mg/mL) and 2 mL sodium-pyruvate (1 mg/mL).

HeLa and EMT6/Ro cells were grown as monolayers in tissue culture flasks (Greiner) in Dulbecco's modified Eagle's medium (Biochrom KG, Berlin, FRG) supplemented with 3.7 g/L $NaHCO_3$, 100 mg/L streptomycine sulfate, 150 mg/L penicillin G, and 10% calf serum.

For initiation of multicell tumor spheroids, monolayer cultures were treated with 0.25% trypsin (in phosphate-buffered saline without calcium and magnesium). In 94 mm diameter plastic Petri dishes (Greiner) 1–2 $\times$ 10^6 single cells were then seeded. Within three days, cells aggregated and were then transferred into spinner flasks (Bellco Glass, Vineland, NJ) filled with 60 mL culture medium and cultured at 120 rpm on magnetic stirrers (type EOA-W, IKA-Werk, Staufen, FRG) regulated with a control unit (type ES 5, IKA-Werk). Culture medium was renewed daily and spheroids were screened microscopically for growth and morphology.

All cell cultures were grown at pH 7.4 and 37°C in a humidified incubator with an atmosphere of 8% CO_2 in air.

Shock wave treatment

Shock waves were generated in a XL1 lithotripter (Dornier Medizintechnik GmbH, Germering, FRG) as is shown in Fig. 1. The XL1 lithotripter is an experimental instrument with an HM3 generator. For the Dornier HM3, lithotripter shock wave pressures of up to 38.6 MPa have been measured in the focus at 20 kV discharge potential (Coleman et al. 1987c). The pressure decreases to 50% within 10 mm in the plane perpendicular to major axis and within 60 mm along the major axis (Saunders and Coleman 1987). In the experimental XL1 lithotripter the pressure is about 2$\times$ higher (Dornier Medizintechnik, personal communication). Cell cultures were transferred into test tubes (polyethylene pipettes, length of pipette ball: 4 cm, diameter: 1.3 cm; Renner GmbH, Darmstadt, FRG), positioned into F_2 and exposed to different SW doses.

For treatment with SW and subsequent histological investigation, L1210 cells were pelleted by centrifugation (10 s, 1000 g), resuspended in culture medium and transferred into the test tubes at a density of 1.2 $\times$ 10^6 cells per mL. A test tube with control cultures was kept in a water bath at 37°C, identical to the temperature of the lithotripter water bath.

Multicell tumor spheroids were washed twice, resuspended in phosphate buffered saline and transferred into the test tubes, where the spheroids rapidly sedimented. For the application of SW, either the central area or the bottom of the test tube was positioned into F_2.

In another set of experiments multicell tumor spheroids were immobilized either in a solution of 2.5% agar (Serva Feinbiochemika, Heidelberg, FRG) in culture medium or in a 12% solution of purified gelatine (Merck, Darmstadt, FRG), polymerized by submersion of the test tube in ice-cold water for up to 3 min.

To avoid liquefaction of the gelatine mixture, the temperature of the lithotripter water bath was shifted to 21°C.

Under these conditions, spheroids of three different areas of the test tube relative to F_2 could be investigated after SW treatment.

Histology

Cell suspensions as well as suspended or immobilized multicell tumor spheroids were fixed for light- and/or electronmicroscopical histology. Spheroids immobilized in gelatine were recovered by liquefying the gel at 37°C. Agar gels with immobilized spheroids, however, were cut into small cubes, but subsequently processed in the same way as the other cells.

For light microscopical histology, cells were fixed in Bouin-solution for 2 h at room temperature, followed by dehydration in 70% ethanol for 2–3 h, 80% and 96% isopropanol for 30 min at room temperature, and in 100% isopropanol (replaced three times) for 90 min at 45°C. Cells were then impregnated overnight at 57°C in a mixture of equal parts isopropanol and the embedding medium Paraplast Plus (Polyscience, Warrington, PA) and infiltrated for 2 $\times$ 7 h at 57°C with pure Paraplast Plus, followed by embedding in Paraplast Plus. All specimens were cut to 5 μm sections and stained with hematoxylin/erythrosin (Chroma, Köngen, FRG).

For electron microscopical histology, cell cultures were fixed in 2.5% glutaraldehyde (Merck, Darmstadt, FRG) in 0.1 M PBS at pH 7.1 for 2–3 h at room temperature. Postfixation in 1% osmiumtetroxide (Merck) in 0.1 M PBS for 1 h at room temperature was followed by dehydration in ethanol (7 min in 40-, 50-, 60-, 70-, and 80% ethanol, 2 $\times$ 15 minutes in 96- and 100% ethanol) and propylene oxide (2 $\times$ 15 minutes). After impregnation with 2:1 and 1:1 mixtures of propylene oxide and the epoxy resin

Glycidether 100 (formerly Epon 812, C. Roth, Karlsruhe, FRG), as well as with pure epoxy resin, cells were embedded in gelatine capsules and polymerized for 12 h at 40°C and 48 h at 70°C. Specimens were thin sectioned with a diamond knife on a Reichert OM U3 ultramicrotome (Reichert-Jung, Nußloch, FRG), stained with uranyl acetate and lead citrate and examined with a Zeiss EM 10A electron microscope at 60 kV.

RESULTS

During exposure of L1210 cell suspensions to SW, cells were vigorously agitated and accelerated in the test tube with each shock wave. Controls and cell suspensions exposed to 500 SW were pelleted by centrifugation and fixed for histology within 10 min after shock wave treatment. In the electron microscope, control cultures revealed cells with a rather smooth surface and few microvilli, irregularly shaped nuclei and numerous mitochondria (Fig. 2a).

In pellets of SW-treated cells various pathological alterations could be detected (Fig. 2b). Figure 2c shows a cell with an undulated shape, occurrence of cavities in the cytoplasm and ruptured mitochondrial ultrastructure. The cell in Fig. 2d exhibits swelling of the mitochondria, cytoplasmic cavities and a separation of the cytoplasm from the nucleus with formation of perinuclear cisternae, the latter also shown—in considerably larger size—in Fig. 2e. In addition, numerous cells appeared electron-lucent, with ruptured cell membranes and perinuclear cisternae (Fig. 2f). Apart from these defects observed in geometrically intact cells, a large amount of cell fragments and cellular debris could be detected, as illustrated in Fig. 2b. Since the LD_{50} for L1210 cells is about 500 SW (Brümmer et al. 1989), it is not surprising that many cells could not be distinguished from untreated cells.

In another set of experiments, we cultured three-dimensionally growing multicell tumor spheroids of epithelioid HeLa cells.

In these HeLa spheroids, cells were densely packed, linked by numerous desmosomes and tight junctions with an outer cell layer exhibiting epithelial cell arrangement (*e.g.*, see Fig. 5c). In phase contrast microscopy and light microscopical sections, these spheroids revealed smooth, well-defined borders (Fig. 3a, b, c). In the test tube, spheroids in suspension rapidly sedimented and formed a pellet. For shock wave exposure the pellet was positioned in F_2. With each shock wave, spheroids were vigorously accelerated, thereby subject to shearing forces and collisions. In spheroids treated with 100 SW serious defects in the outer regions could be detected in phase contrast microscopy (Fig. 3d). The loss of numerous cells of the outer cell layers resulted in irregular spheroid borders and occurrence of suspended single cells and cell groups. After application of 300 SW, the amount of spheroid fragments and single cells significantly increased, the remaining spheroids were of irregular shape and size and exhibited severe damage (Fig. 3e). Exposure to 500 SW resulted in a disintegration of the majority of spheroids and an accumulation of small spheroid fragments and single cells (Fig. 3f). Histological sections through the few remaining spheroids revealed serious damage (Fig. 3g). Large spheroids with a necrotic core surrounded by layers of viable cells (see Fig. 3b, c) were damaged to a higher extent than small spheroids which had not yet developed a necrotic core. Very often, large spheroids were broken resulting in a complete loss of the necrotic core. Damage of spheroids in suspension after exposure to 500 SW, however, was considerably reduced if the spheroid pellet in the test tube was positioned 2 cm below F_2. In these experiments, agitation of spheroids during shock wave treatment was extremely rare, and histological sections (Fig. 3h) revealed much less damage in these spheroids compared to the above described experiments.

In a different experimental approach, we circumvented acceleration and collisions of the spheroids during SW treatment by immobilisation in an agar or gelatine matrix. This allowed a histological investigation of the immobilized spheroids in defined positions relative to F_2. Whereas spheroids in a polymerized agar matrix could not be resuspended for further light microscopical or histological investigation, but had to be processed in small agar cubes, spheroids immobilized in gelatine could be recovered by liquefaction of the gelatine mixture at 37°C. After exposure to 500 SW, no defects could be detected in light microscopical histology regardless of the position of the immobilized spheroids relative to F_2 (upper, middle, or lower third of the test tube, with the middle third positioned into F_2). Even large spheroids with a necrotic center, which were subject to most serious damages when exposed as suspension to 500 SW, did not exhibit any defects (Fig. 3c).

Under the electron microscope, spheroids in suspension treated with 500 SW in F_2 exhibited severe cellular damage in the outer regions of the spheroids (Fig. 4a), similar to those described for shock wave treated L1210 cell suspensions. At the cellular level, vacuolisation of the cytoplasm and ruptures of the mitochondrial fine structure was apparent, desmosomes, however, were unaffected (Fig. 4b). Serious cellular defects like the occurrence of large vacuoles in the cytoplasm, partial disappearance of polyribosomes, and dramatic pathological alterations of the

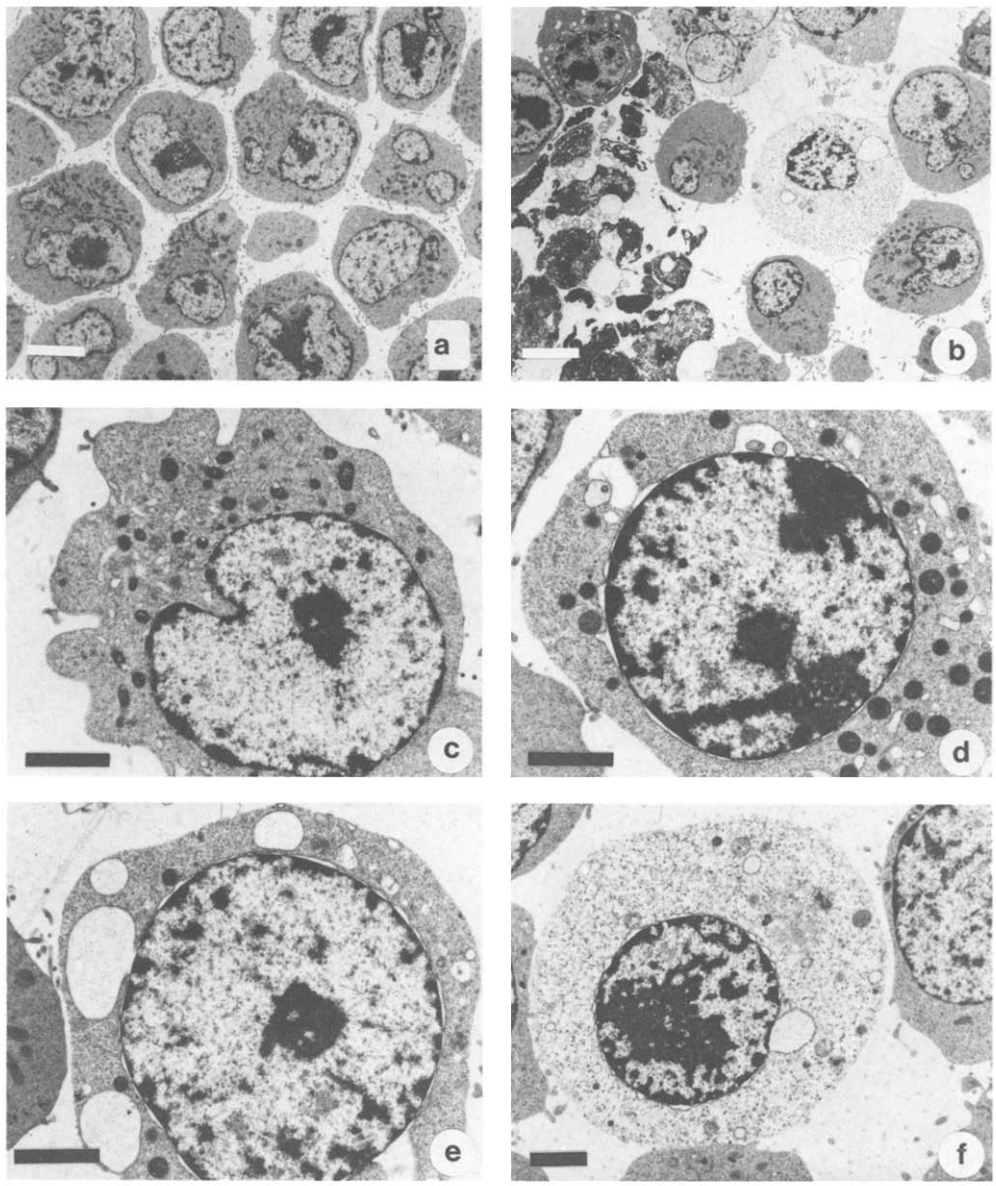

Fig. 2. Electron micrographs of L1210 mouse leukemia cells in suspension. Control cultures (a) and cell suspensions treated with 500 SW (b–f). (a) Control cells exhibit nuclei of irregular shape, numerous mitochondria and few microvilli. (b) SW-exposed cells in low magnification overview: intracellular damage and cell fragmentation. (c) Alteration of cell shape, swollen mitochondria, vacuolisation of the cytoplasm. (d) Swelling of mitochondria, occurrence of perinuclear cisternae and vacuolisation of the cytoplasm. (e) Large perinuclear and cytoplasmic cisternae. (f) Electron-lucent cell with ruptured cell membrane and perinuclear cisternae. Bar: 5 μm (a, b); 2 μm (c–f).

mitochondrial fine structure is shown in the electron-lucent cell in Fig. 4c.

In contrast, SW-treated immobilized spheroids revealed intact epithelial cell arrangements (Fig. 5a), unaffected mitochondrial fine structures (Fig. 5b), and intact desmosomes, thus not differing from untreated control spheroids embedded in gelatine (Fig. 5c). The same results were obtained with SW-treated spheroids immobilized in agar.

Similar experiments were carried out with multicell tumor spheroids of fibroblastioid EMT6/Ro cells. The pattern of cell packing in these spheroids was quite different from that observed in HeLa spheroids. The fibroblastioid EMT6/Ro cells were less densely arranged (Fig. 7c) and exhibited fewer desmosomes and no tight junctions. Exposure of EMT6/Ro spheroids in suspension to 500 SW also resulted in partial destruction, mainly in the outer

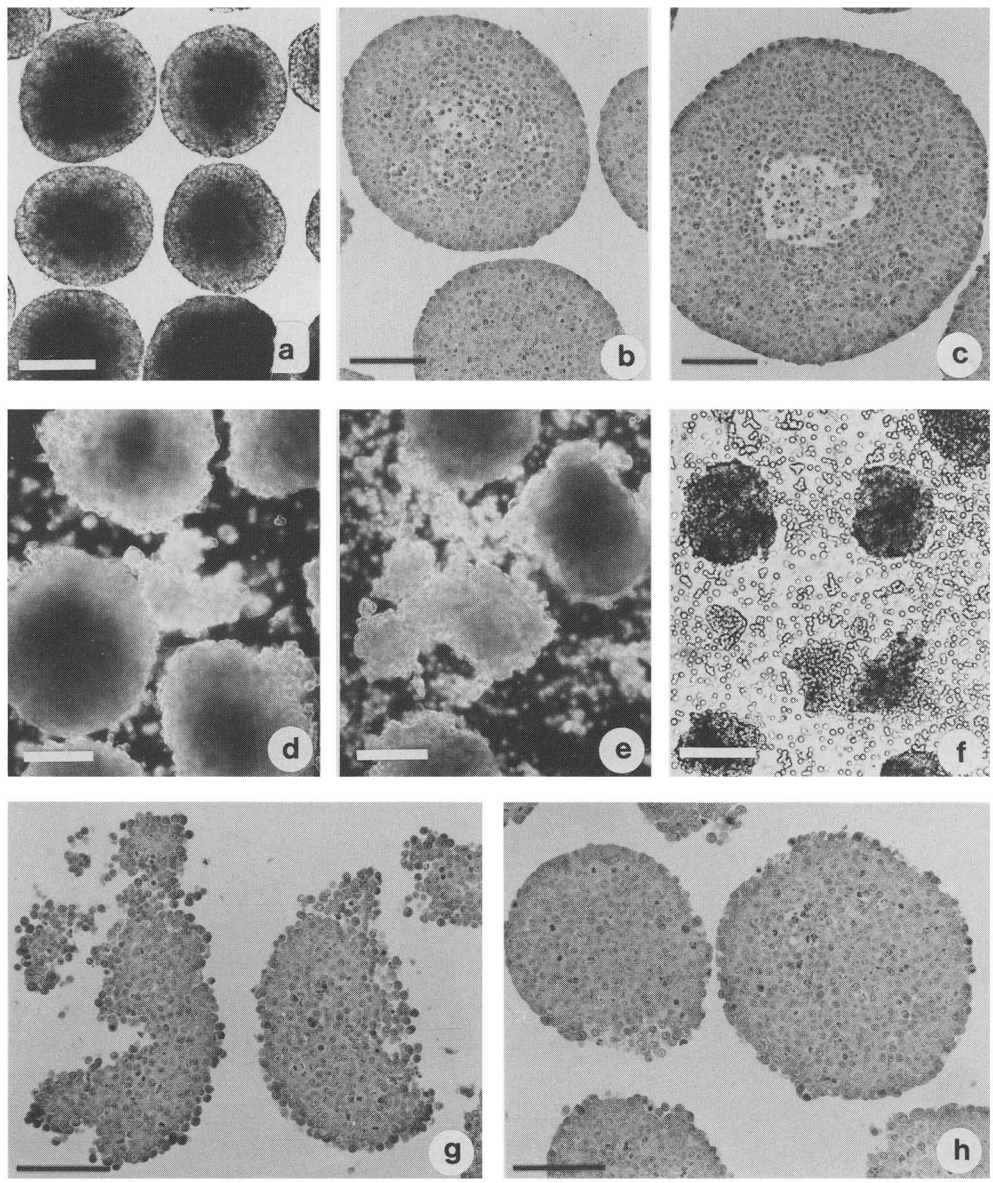

Fig. 3. Multicell tumor spheroids of the human cervix carcinoma line Hela under different experimental conditions. (a) Untreated spheroids under phase contrast illumination. (b) Section through a control spheroid. (c) Section through a spheroid immobilized in gelatine and treated with 500 SW. (d), (e), (f) Spheroids in suspension, treated with 100, 300 and 500 SW, respectively; spheroid pellet positioned in F_2; dark field (d, e) or phase contrast (f) illumination. (g) Section through spheroids in suspension, treated with 500 SW; spheroid pellet positioned in F_2. (h) Section through spheroids in suspension, treated with 500 SW; spheroid pellet positioned 2 cm below F_2. Bar: 200 μm (a, d, e, f); 100 μm (b, c, g, h).

regions (Fig. 6a). Compared to the experiments with HeLa spheroids, however, total fragmentation of EMT6/Ro spheroids was less frequent. At the cellular level electron-lucent appearance of the cytoplasm, extensive vacuolisation, rupture of mitochondria and large perinuclear cisternae could be observed (Fig. 6b, c). After immobilisation of the spheroids in gelatine and subsequent treatment with 500 SW, spheroid size and morphology appeared unaffected in light microscopical histology (Fig. 7a). Electron microscopical sections revealed no difference in the cells' ultrastructure between SW-treated spheroids immobilized in gelatine (Fig. 7b) and untreated spheroids (Fig. 7c).

DISCUSSION

Shock waves generated by underwater spark discharge have been shown to reduce viability and col-

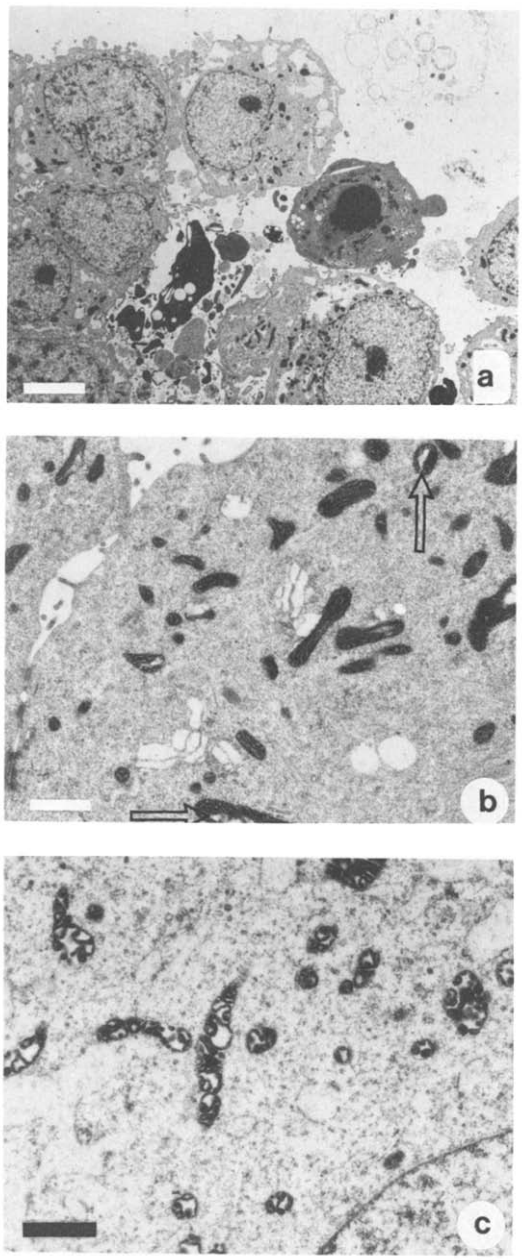

Fig. 4. Electron micrographs of HeLa spheroids in suspension, positioned in F_2 and treated with 500 SW. (a) Cellular damage in the outer region of a spheroid. (b) Ruptures of the mitochondrial fine structure (arrows) and vacuolisation in a cell at the outer region of the spheroid. (c) Electron-lucent cell with large vacuoles and severe pathological alterations of the mitochondrial fine structure. Bar: 5 μm (a); 1 μm (b, c).

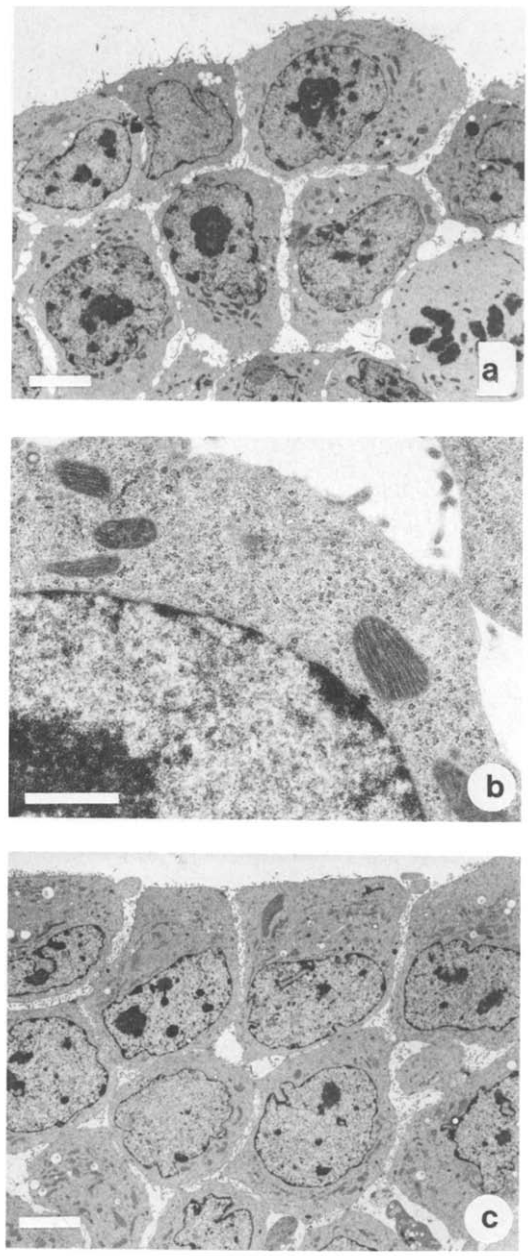

Fig. 5. Electron micrographs of HeLa spheroids immobilized in gelatine and exposed to 500 SW in F_2 (a, b); control (c). (a) Spheroid with intact cellular arrangement and morphology. (b) Cells in the outer region of the spheroid reveal unaffected ultrastructure. (c) Untreated spheroid (control) exhibiting the epithelial arrangement of cells. Bar: 5 μm (a, c); 1 μm (b).

ony formation capacity of rat prostatic carcinoma cells and human melanoma cells treated as single cell suspensions (Russo et al. 1986). These cell lines exhibited differences in the susceptibility to the cytotoxic effects of shock waves. Histological investigations on shock wave treated tumor cell suspensions revealed cell fragmentation or pathological alterations, such as swollen mitochondria with distorted cristae, whereas *in vivo* exposure of tumor nodules to shock waves did not cause specific histopathological effects (Russo et al. 1987). After *in vivo* exposure to shock waves, however, a growth delay of tumor nod-

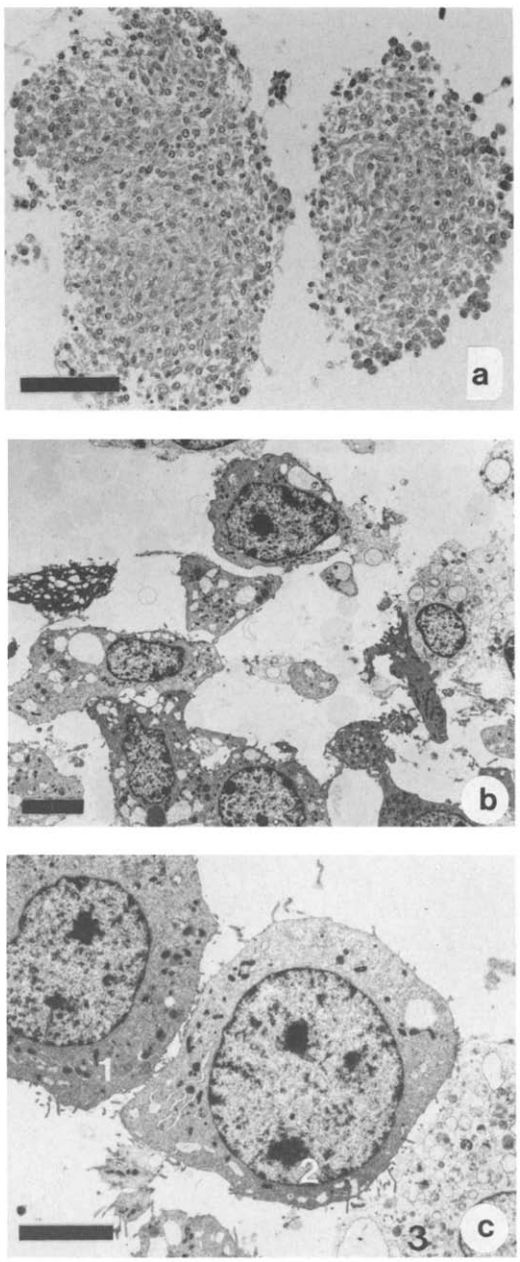

Fig. 6. Light and electron micrographs of multicell tumor spheroids of the mouse mammary tumor line EMT6/Ro in suspension, exposed to 500 SW in F_2. (a) Destruction of the outer cell layers with loss of numerous cells or cell groups. (b) Cellular organization in the outer regions of the spheroid is severely affected, with cells exhibiting large cytoplasmic vacuoles. (c) Various degrees of cellular damage: vacuolisation of the cytoplasm (1), cytoplasmic vacuoles and ruptures in mitochondria (2), and large vacuoles in a permeabilized, electron-lucent cell (3). Bar: 100 μm (a), 5 μm (b, c).

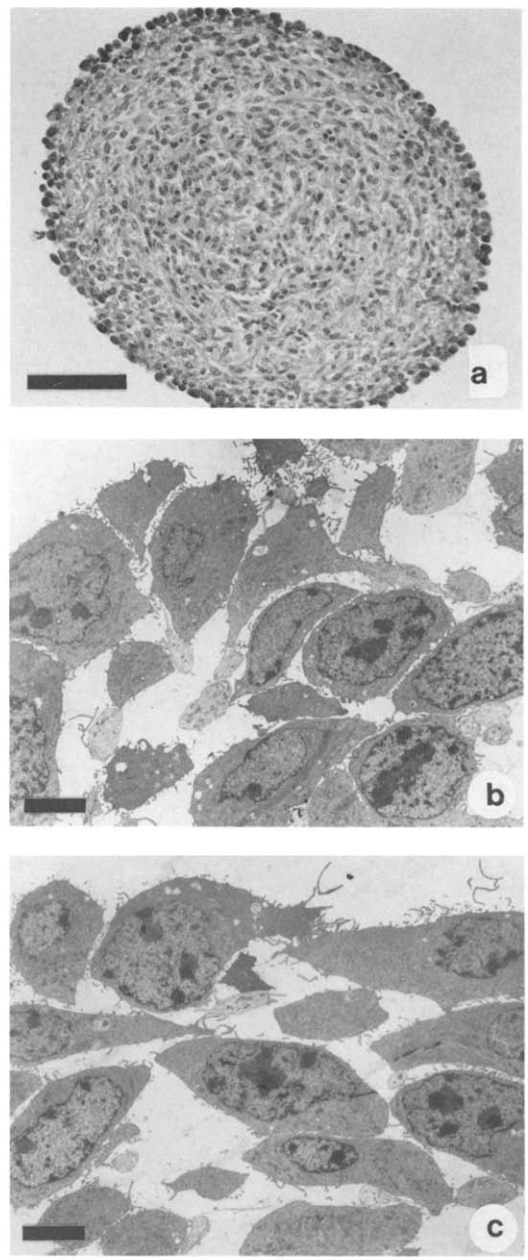

Fig. 7. Light- and electron micrographs of EMT6/Ro spheroids immobilized in gelatine and exposed to 500 SW in F_2 (a, b); control (c). (a) Spheroid reveals intact cellular organization. (b) Cell morphology is unaffected at the ultrastructural level. (c) Untreated spheroid (control). Bar: 100 μm (a); 5 μm (b, c).

ules was observed which may point to a possible application in tumor therapy (Russo et al. 1986). This discrepancy indicates the need for a further characterization of the mechanism of shock wave induced cytotoxicity.

Our earlier studies on the effect of shock waves on L1210 mouse leukemia cell suspensions (Brümmer et al. 1989) revealed a dose-dependent decrease in the number of intact cells with a 50%-loss of cells after application of 500 SW. In these experi-

ments, however, the population of intact cells contained subpopulations of nonviable cells as determined with a double staining technique and flow cytometry.

These results correlate well with our histological investigations shown in the present paper. L1210 cells which appeared to survive treatment with 500 SW as intact cells (*i.e.*, their volume fitted the values measured with untreated cells) frequently exhibited pathological alterations of the cell shape, cell membrane, and cell organelles. This subpopulation of cells may be identical with the cells detected as geometrically intact but nonviable in flow cytometry measurements (Brümmer et al. 1989). The most prominent histopathological alterations such as cytoplasmic cavities occurred due to considerable dilatations of the endoplasmic reticulum. As the endoplasmic reticulum is known to be continuous with the outer nuclear membrane, its dilatation also accounts for the large perinuclear cavities observed in SW-treated cells. Very often, these pathological phenomena were associated with either swelling of the mitochondria or distortion of the mitochondrial cristae. Rupture of the cell membrane causing cell leakage may account for the electron-lucent appearance quite often detected in SW-treated cell suspensions. A substantial fraction of cells treated in suspensions with 500 SW, however, could not be distinguished histologically from untreated cells. These results correspond well with our previous experiments, in which unaffected cell proliferation was demonstrated for about 80% of the geometrically intact cells after treatment with 500 SW (Brümmer et al. 1989).

In further experiments we exposed suspensions of multicell tumor spheroids to shock waves. Revealing a higher rate of survival after ultrasonic treatment than cell suspensions or monolayer cultures, multicell spheroids have been shown to be closer to the conditions of solid tissue *in vivo* (Sacks et al. 1981). This increased survival was thought to occur due to a cellular stabilization in multicell structures such as spheroids, where cells establish the normal cell-to-cell contacts and junctional complexes. Our experiments in which suspensions of multicell tumor spheroids were treated with shock waves revealed both dose-dependent damage and cell-line-specific susceptibility. Spheroids of epithelial HeLa cells exhibit a high cellular packing density with numerous tight junctions between adjacent cells, which seal the intercellular space, thus causing diffusion barriers which contribute to the early occurrence of central necrosis (Bräuner 1987). In large HeLa spheroids with a diameter >500 μm a necrotic core occurs surrounded by vital cell layers. This inhomogeneity may partly account for the severe damage observed after shock wave treatment, when HeLa spheroids were broken and very often revealed a loss of the central necrotic area.

Under the same experimental conditions, damage in EMT6/Ro spheroids was less severe, in most cases peripheral cell layers were affected, whereas a total rupture of spheroids was rare. In multicell spheroids of the fibroblastioid EMT6/Ro cells tight junctions were absent and intercellular space was considerably larger than in HeLa spheroids. With increasing size, these spheroids also exhibited central necrosis, however, a well defined transition between viable cells and necrosis as revealed by HeLa spheroids could not be detected. These histological data indicate differences in the viscoelastic properties of HeLa and EMT6/Ro spheroids. As spheroids in suspension were subject to jet streams causing considerable acceleration and shearing forces as well as numerous collisions during shock wave exposure, a higher rigidity of HeLa spheroids may account for the more severe damage observed in these spheroids.

For suspensions of both HeLa and EMT6/Ro spheroids, histopathological effects of shock wave treatment strongly depended on the position of the spheroid pellet relative to F_2. Positioning of the spheroids 2 cm below F_2 resulted in a striking reduction of spheroid agitation during shock wave treatment. Consequently, these spheroids exhibited much less damage compared with the above described spheroids, which were positioned in F_2. These experiments indicate a major influence of secondary shock wave effects such as jet streams, shearing forces, and collisions on multicell spheroids.

Interestingly, liquid jet impacts resulting from cavitation bubble collapse have been shown to cause damage on various target surfaces placed near F_2 in a Dornier lithotripter (Coleman et al. 1987b). In addition jet streams may also occur due to a local acceleration of the fluid induced by focused SW (Müller 1987). Additional evidence for the key role of jet-stream-associated secondary effects on cell and spheroid damage was derived from experiments in which multicell spheroids were embedded in agar or gelatine. In these matrices jet streams are no longer possible and cavitations do not occur as has been demonstrated in gelatine blocks (Brümmer et al. 1988). Our histological investigation of immobilized HeLa and EMT6/Ro multicell spheroids after exposure to 500 SW in various positions relative to F_2 did not reveal pathological alterations. These histological results are in good agreement with measurements of the physiological condition of L1210 cells immobilized in gelatine and exposed to SW (Brümmer et al.

1989). In these experiments, a dose-dependent damage of L1210 cells, as observed with cells in suspension at the same temperature, could no longer be detected.

In conclusion, our present data provide further evidence that damage observed after SW-treatment of single cells or multicell spheroids in suspension can be attributed to secondary effects, such as jet streams (of cavitational and non-cavitational origin), which cause acceleration and shearing forces and cell/spheroid collisions.

This interpretation may help to explain the—at first sight—contradictory results of Russo and coworkers (1987), who described fragmentation or severe pathological alterations in SW-treated tumor cell suspensions, whereas the *in vivo* exposure of solid tumor nodules did not cause specific histopathological effects. With regard to cellular organisation and viscoelastic properties, these solid tumor nodules may well correspond to our multicell tumor spheroids immobilized in agar or gelatine. In both cases, the above described secondary SW-effects are absent, thus no damage was detectable.

Our conclusion may also be applicable for the interpretation of complications observed after clinical SW treatment. These side effects mainly comprise petechial bleedings of the skin (Eisenberger and Rassweiler 1986) and subcapsular or diffuse hemorrhages (Grote et al. 1986; Baumgartner et al. 1987), whereas severe histopathological alterations of SW-treated kidneys were not described. Again secondary SW-effects occurring in fluids may account for the damage in small capillaries and interstitial cavities. In solid kidney tissue, however, these secondary effects cannot occur, thus explaining the lack of histopathological alteration in treated kidneys.

Acknowledgment—The excellent technical assistance of Ms. Ulrike Reber and Ms. Beate Rehkopf is greatly appreciated. The authors would like to thank Joachim Brenner for technical advice and helpful discussions.

EMT6/Ro cells were kindly supplied by Prof. Dr. R. M. Sutherland, Rochester, NY, USA.

This work was supported by Dornier Medizintechnik GmbH and Bundesministerium für Forschung und Technologie (0318892 A).

REFERENCES

Baumgartner, B. R.; Dickey, K. W.; Ambrose, S. S.; Walton, K. N.; Nelson, R. C.; Bernardino, M. E. Kidney changes after extracorporeal shock wave lithotripsy: appearance on MR imaging. Radiology 163:531–534; 1987.

Bräuner, Th. Interzelluläre Kommunikation und invasives Wachstum maligner Zellen. Stuttgart: Verlag Stöffler & Schütz; 1987.

Brümmer, F.; Brenner, J.; Bräuner, Th.; Hülser, D. F. Effect of shock waves on suspended and immobilized L1210 cells. Ultrasound Med. Biol. 15:229–239; 1989

Brümmer, F.; Brenner, J.; Bräuner, Th.; Nesper, M.; Hülser, D. F. Einwirkung von Stoßwellen auf tierische Zellkulturen. Durchflußzytometrische Untersuchungen physiologischer Parameter. Biomed. Tech. 33(Suppl. 2):36; 1988.

Chaussy, C.; Brendel, W.; Schmiedt, E. Extracorporeally induced destruction of kidney stones by shock waves. Lancet I:1265–1268; 1980.

Coleman, A. J.; Saunders, J. E.; Palfrey, E. L. H. The destruction of renal calculi by external shock-waves: practical operation and initial results with the Dornier lithotripter. J. Medical Engineering and Technology 11:4–10; 1987a.

Coleman, A. J.; Saunders, J. E.; Crum, L. A.; Dyson, M. Acoustic cavitation generated by an extracorporeal shock-wave lithotripter. Ultrasound Med. Biol. 13:69–76; 1987b.

Coleman, A. J.; Saunders, J. E.; Preston, R. C.; Bacon, D. R. Pressure waveforms generated by a Dornier extracorporeal shock-wave lithotripter. Ultrasound Med. Biol. 13:651–657; 1987c.

Delius, M.; Enders, G.; Yuan, Z.; Liebich, H.-G.; Brendel, W. Biological effects of shock waves: kidney damage by shock waves in dogs—dose dependence. Ultrasound Med. Biol. 14:117–122; 1988.

Eisenberger, F. Fortschritte in der extrakorporalen Stosswellenlithotripsie. Historie, gegenwärtige Gerätephilosophie und klinische Daten. Biomed. Tech. 33:11–12; 1988.

Eisenberger, F.; Rassweiler, J. Extrakorporale Stoßwellenlithotripsie im Wandel. Akt. Urol. 17:229–233; 1986.

Gey, G. O.; Coffman, W. D.; Kubicek, M. T. Tissue culture studies of the proliferative capacity of cervical carcinoma and normal epithelium. Cancer Res. 12:264–265; 1952.

Grote, R.; Döhring, W.; Aeikens, B. Computertomographischer und sonographischer Nachweis von renalen und perirenalen Veränderungen nach einer extrakorporalen Stoßwellenlithotripsie. Fortschr. Röntgenst. 144:434–439; 1986.

Hutchinson, D. J.; Ittensohn, O. L.; Bjerregaard, M. R. Growth of L1210 mouse leukemia cells in vitro. Exp. Cell Res. 42:157–170; 1966.

Müller, M. Stoßwellenfokussierung in Wasser. Aachen, FRG: RWTH; 1987. Ph.D. thesis.

Müller-Klieser, W. Multicellular spheroids. A review on cellular aggregates in cancer research. J. Cancer Res. Clin. Oncol. 113:101–122; 1987.

Rockwell, S. C.; Kallman, R. F.; Fajardo, L. S. Characteristics of a serially transplanted mouse mammary tumor and its tissue-culture-adapted derivate. J. Natl. Cancer Inst. 49:735–749; 1972.

Russo, P.; Stephenson, A.; Mies, C.; Huryk, R.; Heston, W. D. W.; Melamed, M. R.; Fair, W. R. High energy shock waves suppress tumor growth in vitro and in vivo. J. Urol. 135:626–628; 1986.

Russo, P.; Mies, C.; Huryk, R.; Heston, W. D. W.; Fair, W. R. Histopathologic and ultrastructural correlates of tumor growth suppression by high energy shock waves. J. Urol. 137:338–341; 1987.

Sacks, P. G.; Miller, M. W.; Sutherland, R. M. Influences of growth conditions and cell-cell contact on responses of tumor cells to ultrasound. Radiat. Res. 87:175–186; 1981.

Saunders, J. E.; Coleman, A. J. Physical characteristics of Dornier extracorporeal shock-wave lithotripter. Urology 24:506–509; 1987.

Scherer, W. F.; Syverton, J. T.; Gey, G. O. Studies on the propagation in vitro of poliomyelitis viruses. IV. Viral multiplication in a stable strain of human epithelial cells (strain HeLa) derived from an epidermoid carcinoma of the cervix. J. Exp. Med. 97:695–709; 1953.

Sutherland, R. M.; McCredie, J. A.; Inch, W. R. Growth of multicellular spheroids in tissue culture as a model of nodular carcinomas. J. Natl. Cancer Inst. 46:113–120; 1971.

Sutherland, R. M. Cell and environment interactions in tumor microregions: the multicell spheroid modell. Science 240:177–184; 1988.